JPEDAV (2006) 27:343-352
DOI: 10.1361/154770306X116270
1547-7037/$19.00 ©ASM International

Thermodynamic Database for the ZrO_2-$YO_{3/2}$-$GdO_{3/2}$-$AlO_{3/2}$ System and Application to Thermal Barrier Coatings

O. Fabrichnaya, S. Lakiza, Ch. Wang, M. Zinkevich, C.G. Levi, and F. Aldinger

(Submitted January 15, 2006; in revised form March 3, 2006)

The thermodynamic database for the ZrO_2-$YO_{3/2}$-$GdO_{3/2}$-$AlO_{3/2}$ system is integrated from ternary descriptions. The liquidus surface and isothermal sections are calculated for the ZrO_2-free subsystem, which has not yet been studied experimentally. Calculated quaternary isoplethal sections with fixed $GdO_{3/2}$ and $YO_{3/2}$ content are reported. The influence of the total content of stabilizers, (Y + Gd), and the Y/(Gd + Y) ratio on the phase relations is demonstrated. The T_0-curves for the diffusionless transitions fluorite ↔ tetragonal and tetragonal ↔ monoclinic are calculated for binary and ternary ZrO_2 compositions of interest in thermal barrier coatings (TBC). The driving force for the partitioning of metastable fluorite and tetragonal phases to the equilibrium two-phase assemblage is calculated at various compositions and temperatures for the ZrO_2-$GdO_{3/2}$-$YO_{3/2}$ system and its implications for TBCs are discussed.

Keywords partially stabilized zirconia, phase diagrams, thermal barrier coatings, thermodynamic modeling, zirconates

1. Introduction

An important group of emerging thermal barrier coating (TBC) materials for advanced gas turbines is based on additions of Gd^{3+} to ZrO_2, either as a single dopant,[1,2] in combination with the more established Y^{3+} stabilizer,[3] or in more complex codoped formulations involving Sc^{3+} and/or other lanthanide ions, for example, Yb^{3+}.[4] Development of these novel TBC compositions is primarily driven by their lower thermal conductivity and more sluggish sintering kinetics than the currently used 7YSZ (ZrO_2 partially stabilized with 7 to 8 mol% $YO_{3/2}$).[5] The attendant benefits to the thermal insulation efficiency and stability of the coating enable in principle higher performance and durability of the coated engine components, but issues arise with the thermodynamic stability of the coating systems as these novel compositions are introduced.

Arguably the most significant departure from the conventional 7YSZ is manifested in TBCs based on pyrochlore zirconates, of which $Gd_2Zr_2O_7$ is a prime example. In general, all TBCs in current practice attach to the metal "substrate" via a thermally grown oxide (TGO), consisting of nearly pure α-Al_2O_3 that evolves during service and provides oxidation protection to the underlying component. Because all dopants of interest in ZrO_2 form compounds with Al_2O_3, one can readily show that above a critical composition the TBC would tend to react with the TGO to form an interphase, usually degrading the adhesion and the efficiency of the TGO as a diffusion barrier.[5] Indeed, this reaction has been demonstrated for $Gd_2Zr_2O_7$ with appreciable rates above ~1100 °C,[6] but the problem can be circumvented either by controlling the temperature of the TGO/TBC interface to minimize the interaction kinetics, or by interposing an interlayer of a material compatible with both $Gd_2Zr_2O_7$ and the TGO.[5,7]

Codoped compositions can be designed to avoid the thermochemical incompatibility with the TGO, but those that have significant durability perform optimally only when deposited as a supersaturated, metastable tetragonal solid solution (t′) with sufficient stabilizer to render it nontransformable to monoclinic. Hence, upon prolonged exposure to sufficiently high temperatures these compositions tend to relieve their supersaturation by precipitating a stabilizer-rich cubic phase, leaving behind a depleted tetragonal matrix that becomes transformable to the disruptive monoclinic under thermal cycling. Rebollo et al.[8] found that t′-ZrO_2 stabilized by Gd alone is less resistant to partitioning at high temperature than its Y counterpart with the same concentration. However, oxides with comparable or improved stability could be produced by properly tailoring the relative amounts of Y and Gd.

The previous discussion highlights the importance of understanding the phase relations in the ZrO_2-$YO_{3/2}$-$GdO_{3/2}$-$AlO_{3/2}$ system to guide the design of TBC systems with the desirable stability. The aim of this study is to derive the thermodynamic database for the quaternary system and to use it for calculations of the phase diagrams, the associated T_0 curves, and the driving forces for the partitioning of metastable solid solutions, all of which are relevant to TBC applications.

The thermodynamic descriptions of the ternary systems ZrO_2-$GdO_{3/2}$-$AlO_{3/2}$, ZrO_2-$YO_{3/2}$-$AlO_{3/2}$, and ZrO_2-$YO_{3/2}$-$GdO_{3/2}$ were derived in previous works,[9-11] respectively. These descriptions are accepted in the current study. A more complicated model is used here to describe the monoclinic zirconia solid solution, allowing for the introduction of a

O. Fabrichnaya, S. Lakiza, Ch. Wang, M. Zinkevich, and **F. Aldinger,** Max-Planck-Institut für Metallforschung, Heisenbergstr. 3, 70569 Stuttgart, Germany; **S. Lakiza,** also, Frantsevich Institute of Materials Science Problems, Kiev, Ukraine; **C.G. Levi,** Materials Dept., University of California, Santa Barbara, CA, 93106-5050. Contact e-mail: fabri@mf.mpg.de.

Table 1 Phases stable in the ZrO_2-$GdO_{3/2}$-$YO_{3/2}$-$AlO_{3/2}$ system

Phase	Model
Fluorite (F) Tetragonal (T) Monoclinic (M)	$(Gd^{3+}, Y^{3+}, Al^{3+}, Zr^{4+})_1(O^{2-}, Va)_2$
Cubic (C) Monoclinic-B (B) Hexagonal (H)	$(Gd^{3+}, Y^{3+}, Zr^{4+})_2(O^{2-}, Va)_1(O^{2-})_3$
Hexagonal-A (A) X-phase (X)	$(Gd^{3+}, Y^{3+})_2\ (O^{2-})_3$
δ-$Zr_3Y_4O_{12}$ (δ)	$(Zr^{4+})_3(Y^{3+})_4(O^{2-})_{12}$
Pyrochlore (Pyr)	$(Gd^{3+}, Zr^{4+})_2(Zr^{4+}, Gd^{3+})_2(O^{2-}, Va)_6$ $(O^{2-})_1(Va, O^{2-})_1$
Monoclinic-LnYAM (LnAM)	$(Gd^{3+}, Y^{3+})_4(Al^{3+})_2(O^{2-})_9$
Perovskite-LnAP (LnAP)	$(Gd^{3+}, Y^{3+})_1(Al^{3+})_1(O^{2-})_3$
Garnet-LnAG (LnAG)	$(Gd^{3+}, Y^{3+})_3(Al^{3+})_5(O^{2-})_{12}$
Corundum Al_2O_3	$(Al^{3+})_2(O^{2-})_3$
Liquid (L)	$(Gd^{3+}, Y^{3+}, Zr^{4+})_P(O^{2-}, AlO_{3/2})_Q$

small but finite solubility of $AlO_{3/2}$ and $GdO_{3/2}$, which is necessary to enable calculations of the T_0 curves for the diffusionless tetragonal ↔ monoclinic transition. The system $YO_{3/2}$-$GdO_{3/2}$-$AlO_{3/2}$ had not been previously studied, either experimentally or theoretically. A description of this system is derived in the current study by combining binary descriptions and assuming that the monoclinic (LnAM), perovskite (LnAP), and garnet (LnAG) aluminates (Ln = Y, Gd) form ideal solid solutions. The thermodynamic description of the quaternary system derived here simply combines the ternary descriptions without introducing any quaternary parameters. The goal is to provide guidance for future experimental work that may help refine the description and generate a validated database, as well as to provide insight into the issues relevant to thermal barrier coatings.

2. Thermodynamic Modeling

Phases stable in the system ZrO_2-$YO_{3/2}$-$GdO_{3/2}$-$AlO_{3/2}$, their designation and the thermodynamic models used for their description are presented in Table 1. Most of the solid phases are described by the compound energy formalism.[12] The liquid phase is described by the two-sublattice ionic liquid model[12] with the first sublattice filled by cations and the second one filled by anions, vacancies, and neutral species. This study does not consider the metal-rich part of the system, and vacancies are not included in the liquid description. The liquid is thus described by the formula $(Gd^{3+}, Y^{3+}, Zr^{4+})_P(O^{2-}, AlO_{3/2})_Q$, where P and Q are the number of sites on the cation and anion sublattices, respectively. The stoichiometric factors P and Q vary with the composition to maintain electroneutrality. The remaining phases (corundum and δ-$Zr_3Y_4O_{12}$) are treated as stoichiometric.

Table 2 Thermodynamic parameters for monoclinic ZrO_2 solid solution

Phase: monoclinic; formula: $(Al^{3+}, Gd^{3+}, Y^{3+}, Zr^{4+})_1(O^{2-}, Va)_2$

Parameter	Function
G(ZrO2_M, Al^{3+}:O^{2-})	0.5 · GCORUND + 0.5 · GHSEROO + 100,000 + 9.3511 · *T*
G(ZrO2_M, Gd^{3+}:O^{2-})	0.5 · GGD2O3B + 0.5 · GHSEROO + 50,000 + 9.3511 · *T*
G(ZrO2_M, Y^{3+}:O^{2-})	0.5 · GY2O3R + 0.5 · GHSEROO + 26,900 + 34.7511 · *T*
G(ZrO2_M, Zr^{4+}:O^{2-})	GZRO2M
G(ZrO2_M, Al^{3+}:Va)	0.5 · GCORUND − 1.5 · GHSEROO + 100,000 + 9.3511 · *T*
G(ZrO2_M, Gd^{3+}:Va)	0.5 · GGD2O3B − 1.5 · GHSEROO + 50,000 + 9.3511 · *T*
G(ZrO2_M, Y^{3+}:Va)	0.5 · GY2O3R − 1.5 · GHSEROO + 26,900 + 34.7511 · *T*
G(ZrO2_M, Zr^{4+}:Va)	GZRO2M − 2 · GHSEROO

Functions GCORUND, GHSEROO, GGD2O3B, GY2O3R are from Ref 9 and 11.

The Gibbs energy of a solution phase with mixing in two sublattices (i.e., F, T, M, C, B, A, X, H) is expressed as:

$$G = \sum_i \sum_j Y_i^s Y_j^t G_{i,j} + RT \sum_s \alpha_s \sum_i Y_i^s \ln Y_i^s + \Delta G^{ex} \qquad \text{(Eq 1)}$$

where Y_i^s is the mole fraction of a constituent i in sublattice s, $G_{i,j}$ is Gibbs energy of a compound formed from species i and j, α_s is the number of sites on the sublattice s per mole of formula units of phase and ΔG^{ex} is the excess Gibbs energy of mixing expressed as:

$$\Delta G^{ex} = \sum_s Y_i^s Y_j^s L_{i,j}^s + \Delta G^{tern} \qquad \text{(Eq 2)}$$

where

$$L_{i,j}^s = \sum_n (Y_i^s - Y_j^s)^n L_{i,j} \qquad \text{(Eq 3)}$$

are the binary interaction parameters in the sublattice s and ΔG^{tern} is the contribution of high-order interactions. As a first approximation, the ternary and quaternary interaction parameters for the solid phases are neglected.

In the case of more then two sublattices (i.e., pyrochlore) the Gibbs energy is expressed by:

$$G = \sum G_{end} \prod y_j^s + RT \sum \alpha_s \sum y_j^s \ln y_j^s + \Delta G^{ex} \qquad \text{(Eq 4)}$$

where G_{end} is the Gibbs energy of the end-member compounds. The excess energy for the pyrochlore type phase is assumed to be 0. Modeling of the pyrochlore phase carries some uncertainty because, while it is agreed that the structure is an ordered derivative of fluorite, the nature of the order/disorder transition in the ZrO_2-$GdO_{3/2}$ system is still a subject of debate.[6] Some of the literature suggests a continuous ordering transition between fluorite and pyrochlore, which can be viewed as a hybrid phase containing ordered

Table 3 Invariant reactions in binary systems involving monoclinic phase

Reaction	System	This work, calculated	Calculated in Ref 9,11	Experimental
T = M + F	ZrO_2-$GdO_{3/2}$	T = 1411 K	1410 K	1415[15]
		X(F, $GdO_{3/2}$) = 0.1531	0.1532	
		X(T, $GdO_{3/2}$) = 0.0203	0.0203	
		X(M, $GdO_{3/2}$) = 4.6×10^{-4}	0	
F = Pyr + M	ZrO_2-$GdO_{3/2}$	T = 417 K	417 K	…
		X(F, $GdO_{3/2}$) = 0.3124	0.3124	
		X(M, $GdO_{3/2}$) = 1×10^{-7}	0	
		X(Pyr, $GdO_{3/2}$) = 0.4994	0.4994	
T = M + Al_2O_3	ZrO_2-$AlO_{3/2}$	T = 1403	1397	1423[16]
		X(T, $GdO_{3/2}$) = 0.0262	0.0258	0.02
		X(M, $GdO_{3/2}$) = 2.47×10^{-3}	0	…

and disordered regions.[13,14] In this study, the pyrochlore and fluorite are considered as different phases for the purposes of describing their free energy, and the transformation is assumed to be first order.

3. Results

Introducing a small solubility of $GdO_{3/2}$ and $AlO_{3/2}$ in the monoclinic form of ZrO_2 leads to small changes in the eutectoid reactions T = F + M and F = Pyr + M in the ZrO_2-$GdO_{3/2}$ system and in the eutectoid reaction T = M + Al_2O_3 in the ZrO_2-$AlO_{3/2}$ system relative to previous works. The thermodynamic parameters for the monoclinic phase are presented in Table 2. A comparison of the eutectoid reactions obtained with the new and old descriptions is shown in Table 3, along with experimental data.[15,16] All the other functions are taken from previous descriptions.[9-11]

3.1. Calculation of Phase Relations in the $YO_{3/2}$-$GdO_{3/2}$-$AlO_{3/2}$ System

The ternary system $YO_{3/2}$-$GdO_{3/2}$-$AlO_{3/2}$ is addressed first as no thermodynamic description was previously available for it and such a description is needed for the quaternary ZrO_2-$YO_{3/2}$-$GdO_{3/2}$-$AlO_{3/2}$ database. The thermodynamic parameters of its binary systems, assessed previously[9,11,17] were combined, and the thermodynamic description of the $YO_{3/2}$-$GdO_{3/2}$-$AlO_{3/2}$ system was obtained assuming ideal mixing within the LnAM, LnAP, and LnAG phases, as noted before.

The isothermal sections of the $YO_{3/2}$-$GdO_{3/2}$-$AlO_{3/2}$ system calculated at 1473, 1673, and 1923 K are presented in Fig. 1(a) to (c). Of particular significance is that the garnet (LnAG) phase is destabilized by the addition of Gd, as expected from its absence in the $GdO_{3/2}$-$AlO_{3/2}$ binary. Moreover, the maximum Gd content in the LnAG phase and the minimum Gd content for which direct equilibrium between the perovskite (LnAP) and corundum phases is possible both decrease with increasing temperature. The liquidus surface of this system calculated in the current study is shown in Fig. 2(a) and compared with that predicted by Lakiza[18] in Fig. 2(b).

3.2. Phase Relations in the Quaternary System ZrO_2-$GdO_{3/2}$-$YO_{3/2}$-$AlO_{3/2}$

The thermodynamic description of the quaternary system was derived by extrapolation of the ternaries, without introducing quaternary interaction parameters. The multitude of sections that can be generated from such database is obviously very large. For example, isopleths were calculated for compositions with total stabilizer contents X($GdO_{3/2}$ + $YO_{3/2}$) of 7.6 mol% (Fig. 3a-c) and 15.2 mol% (Fig. 4a-c) and within each series for Y/(Gd + Y) ratios of 0.25, 0.5, and 0.75, which cover the domain relevant to TBCs codoped with Y and Gd. Of particular interest in these figures is the effect of composition on the stability of the ZrO_2 polymorphs,[8] and the conditions under which aluminate phases can form,[6] as discussed later.

3.3. T_0 Curves for the Diffusionless Transitions F ↔ T and T ↔ M

The partitionless transformations between cubic (fluorite) and tetragonal solid solutions, as well as between the tetragonal and monoclinic forms, are of broad relevance in ZrO_2-based materials technology[19-21] and of critical importance in thermal barrier systems.[5] The driving force and thermodynamically favored direction for the transformation depends on the relative position of the system in (T, X_0) space relative to the temperature at which the Gibbs energies of the pair of phases involved are equal for the given composition, designated as (T_0, X_0). By definition these points fall within two-phase fields in the equilibrium diagram, and thus either single phase is metastable within this range relative to the partitioning into the two equilibrium phases, which involves solute redistribution and is generally diffusion controlled. In the quaternary system the locus of the (T_0, X_0) points defines a volume, which reduces to surfaces on the corresponding ternaries and curves on binaries or isopleth sections.

The T_0 curves for the F ↔ T and T ↔ M transitions have been calculated in the binary systems ZrO_2-$YO_{3/2}$, ZrO_2-$GdO_{3/2}$, and ZrO_2-$AlO_{3/2}$ and are presented along with the corresponding phase diagrams in Fig. 5(a) to (c). The calculated T_0 = 703 K for the T ↔ M transition at 5.6 mol% $YO_{3/2}$ is in reasonable agreement with the recently reported experimental value of 648 to 673 K.[22] It should be men-

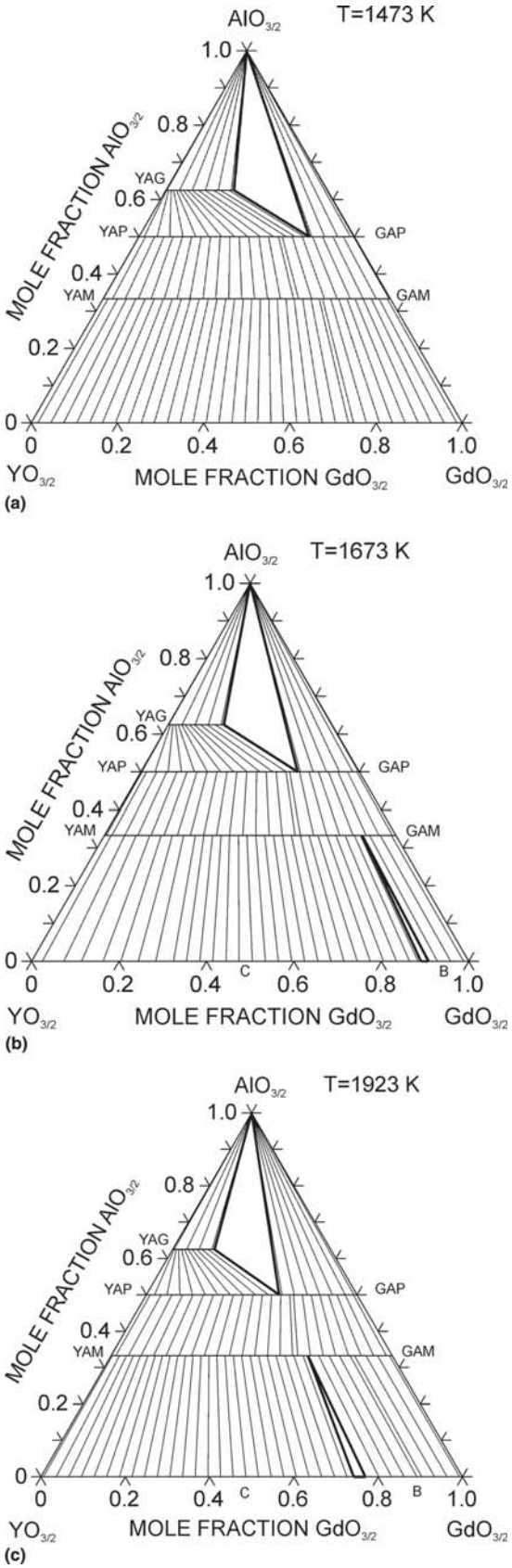

Fig. 1 Isothermal sections of $GdO_{3/2}$-$YO_{3/2}$-$AlO_{3/2}$ system at (a) 1473 K, (b) 1673 K, and (c) 1923 K

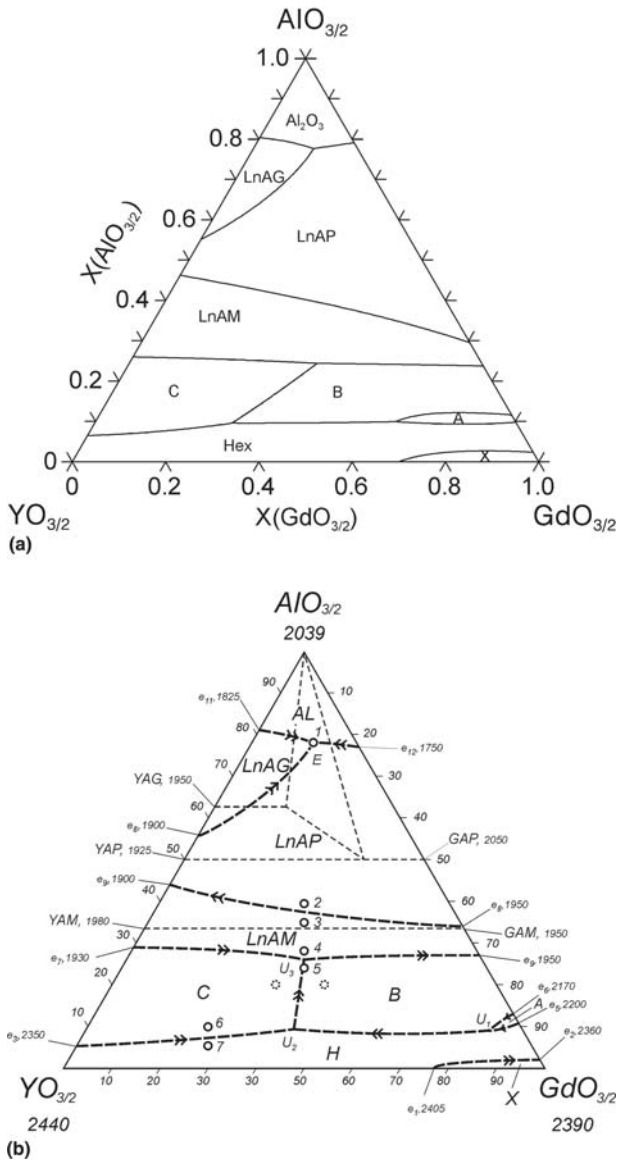

Fig. 2 Liquidus surface of $GdO_{3/2}$-$YO_{3/2}$-$AlO_{3/2}$ system calculated in (a) the present work and (b) predicted by Lakiza

tioned that T ↔ M transition in the pure ZrO_2 occurs as a martensitic one with a hysteresis of about 200 K, and this uncertainty could be a reason for difference in the position of T_0 line for the T ↔ M transition. The consistency between the calculated T_0(F ↔ T) at 12 mol% $YO_{3/2}$ and the experimental value from Yashima et al.[23] is not so good (1342 and 1673 K, respectively). It should be noted, however, that the latter value is ascribed to a t″ ↔ t′ transformation, for which a T_0 temperature should not exist, in principle, because these are not two independent phases. The traces of the T_0 surfaces have also been calculated for the ternary systems ZrO_2-$YO_{3/2}$-$AlO_{3/2}$, ZrO_2-$GdO_{3/2}$-$AlO_{3/2}$, and ZrO_2-$YO_{3/2}$-$GdO_{3/2}$ at different ratios of Y/(Y + Al), Gd/(Gd + Al), and Gd/(Gd + Y). Figure 6(a) to (c) depicts the T_0 traces corresponding to values of the above ratios equal to 0.5, along with the relevant parts of the corresponding ternary isopleths.

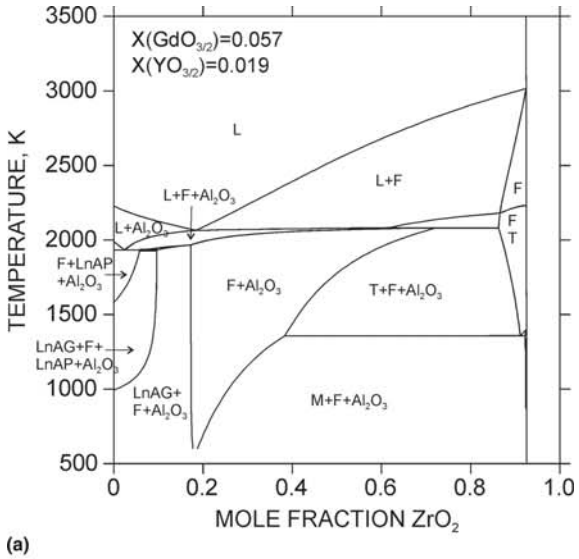

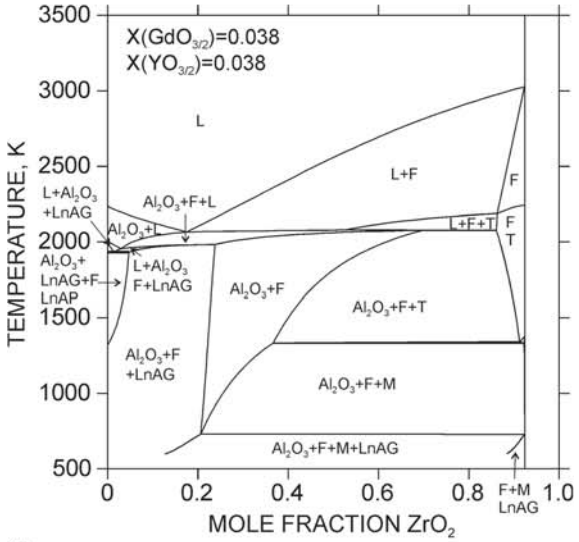

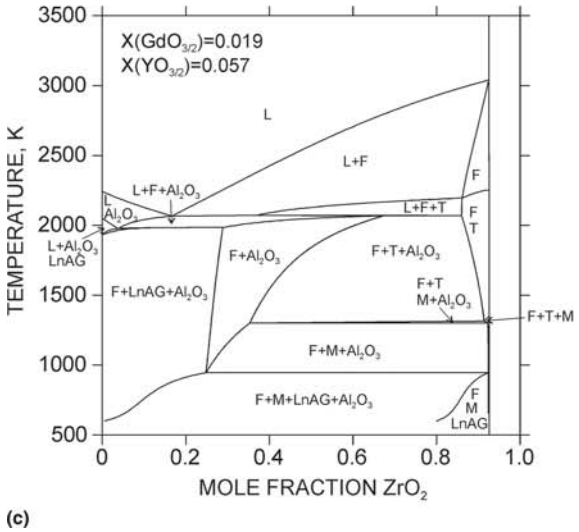

Fig. 3 (a) Phase relations at x(Gd + Y) = 0.076 and Y/(Gd + Y) = 0.25, (b) 0.5, and (c) 0.75

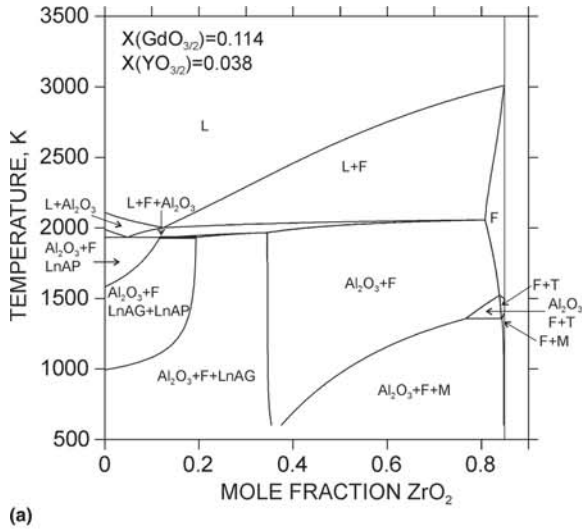

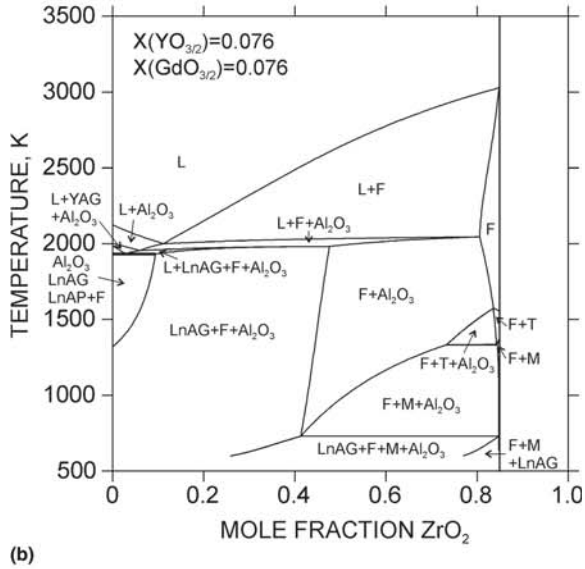

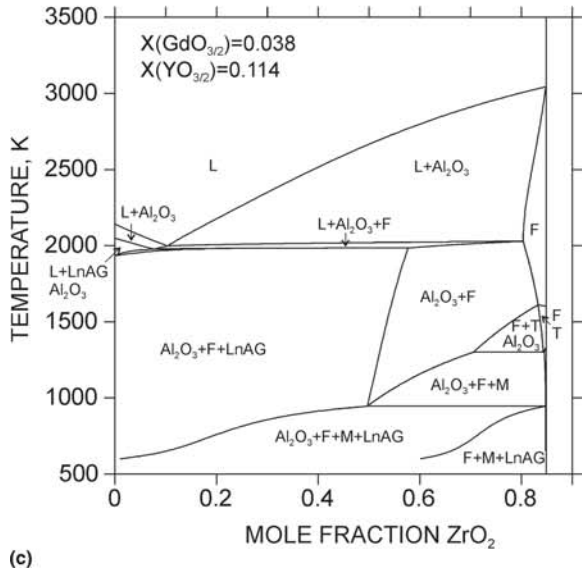

Fig. 4 (a) Phase relations at x(Gd + Y) = 0.152 and Y/(Gd + Y) = 0.25, (b) 0.5, and (c) 0.75

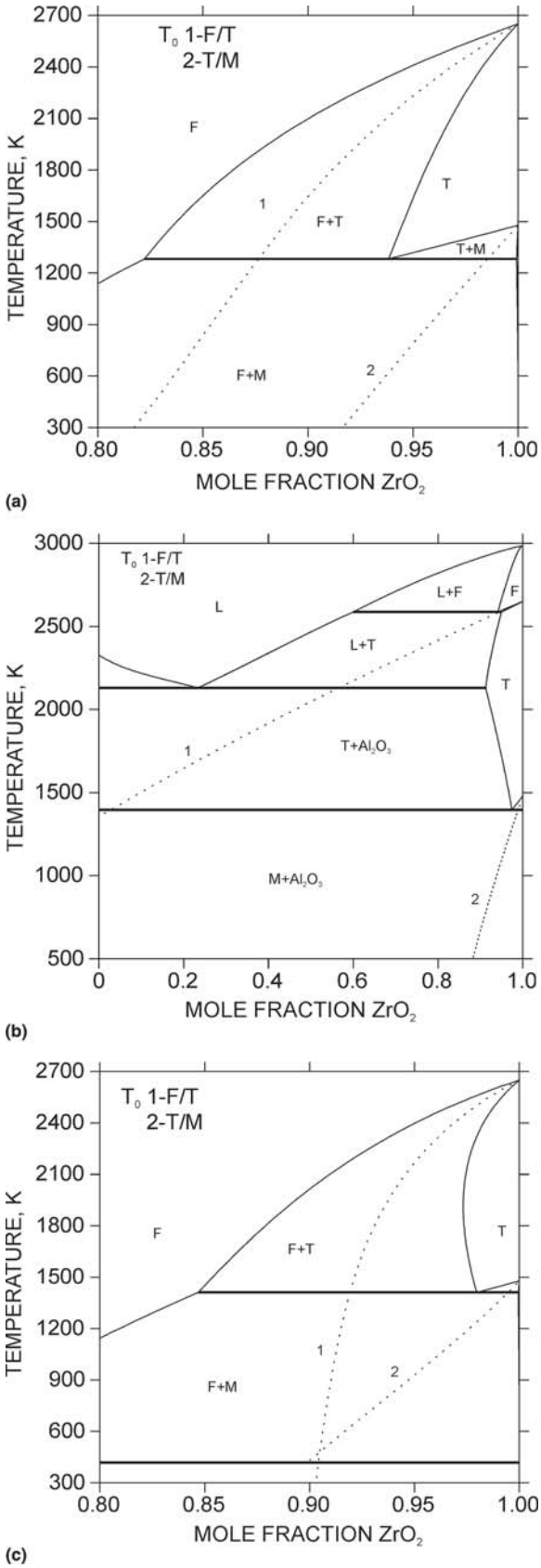

Fig. 5 T_0 lines. (a) In the ZrO_2-$YO_{3/2}$ system. (b) In the ZrO_2-$AlO_{3/2}$ system. (c) In the ZrO_2-$GdO_{3/2}$ system

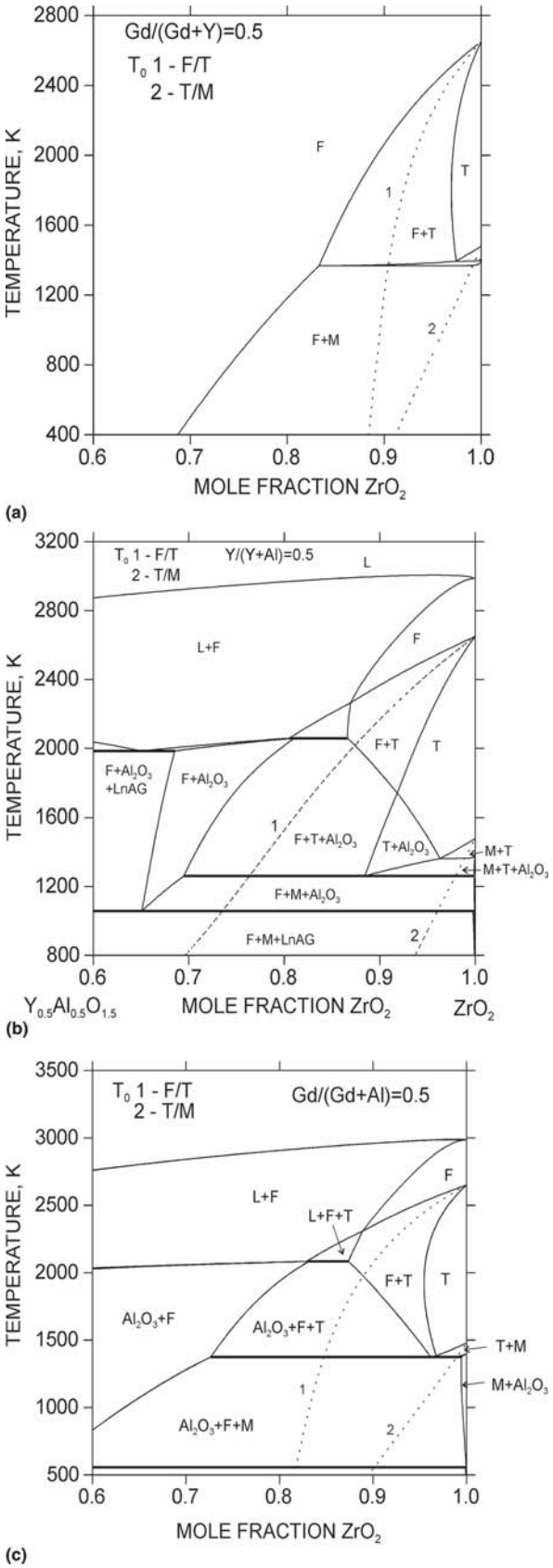

Fig. 6 T_0 lines. (a) In the ZrO_2-$GdO_{3/2}$-$YO_{3/2}$ system. (b) In the ZrO_2-$YO_{3/2}$-$AlO_{3/2}$ system. (c) In the ZrO_2-$GdO_{3/2}$-$AlO_{3/2}$ system

Based on calculations of the T_0(F/T) temperatures at different ratios of the dopant cations one can map the traces of constant T_0(F/T) for the ternary subsystems as illustrated in Fig. 7(a) to (c). These define the composition ranges wherein either the tetragonal or cubic forms can be synthesized as single phases, either stable or kinetically stabilized, at a given temperature.

3.4. Driving Force for Partitioning of Supersaturated Fluorite or Tetragonal Phases

The assembled database is also useful in determining the driving forces that enter into understanding the kinetics of the relevant transformations. These driving forces are readily calculated as the difference in the Gibbs energy of the parent metastable phase and the product assemblage of phases. Of particular relevance to thermal barrier systems are the driving forces for the partitioning of metastable tetragonal and fluorite phases when held into the two phase F + T equilibrium field, because such partitioning leads to the production of a transformable tetragonal phase with deleterious consequences to the integrity of the coating. The driving forces for this partitioning transformation are presented in Fig. 8(a) and (b) for the ZrO_2-$YO_{3/2}$ and ZrO_2-$GdO_{3/2}$ systems in the temperature range 1173 to 1773 K, and for various combinations of Y and Gd within the ternary at 1473 K in Fig. 9. At compositions corresponding to equilibrium, the driving forces are equal to 0. The maximum driving force occurs at the composition wherein the Gibbs energies of the tetragonal and fluorite phases are identical, that is, at the composition corresponding to T_0 line as discussed in work of Rebollo et al.[8]

4. Implications for Thermal Barrier Coatings

The calculations presented in the figures in this article provide insight into a number of issues relevant to thermal barrier coatings. First, it is noted in Fig. 3 and 4 that the fluorite and tetragonal fields are in equilibrium with alumina at all temperatures relevant to TBC applications, confirming the hypothesis that deleterious interphase formation between the TBC and the TGO should not be an issue for typical codoped compositions contemplated in current technology.[6] It is evident, however, that there is nonnegligible solubility of Al^{3+} in F and T, especially at the higher temperatures. The implication is that a thin TGO would tend to gradually dissolve in the much thicker TBC with detrimental effects on its ability to protect the underlying metal against oxidation. This problem has not been reported to date, arguably because the temperature of the TBC/TGO interface is sufficiently low for cation diffusion to be insignificant. However, it is undoubtedly important for interfaces in alumina-zirconia bilayer and multilayer architectures that have been proposed to enhance certain TBC properties such as thermal insulation efficiency,[24] erosion,[25] and corrosion resistance.[26] Comparison of Fig. 3 and 4 at the same Y/(Gd + Y) ratio reveals that increasing the total amount of stabilizer shrinks both the F + T and F + T + Al_2O_3 fields while extending that of F + Al_2O_3 to higher ZrO_2 contents.

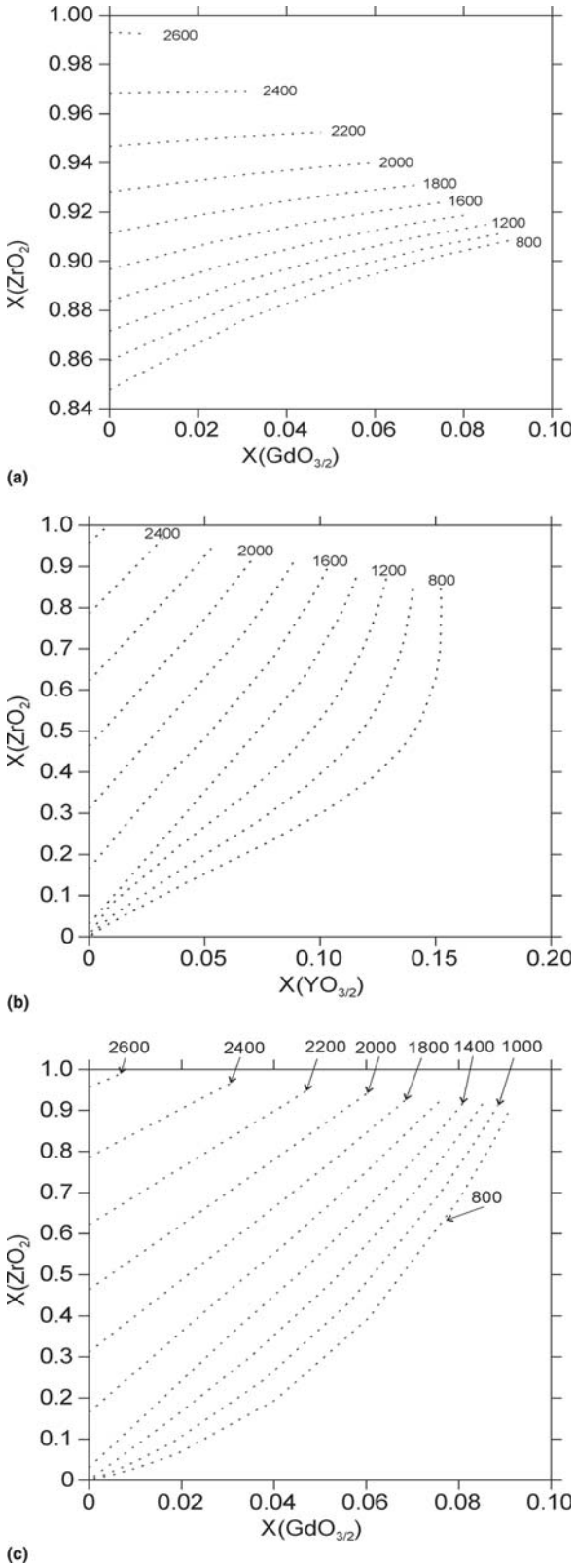

Fig. 7 Iso-T_0 lines (K) of F ↔ T transformation. (a) In the ZrO_2-$GdO_{3/2}$-$YO_{3/2}$ system. (b) In the ZrO_2-$YO_{3/2}$-$AlO_{3/2}$ system. (c) In the ZrO_2-$GdO_{3/2}$-$AlO_{3/2}$ system. Numbers designating curves are temperatures T_0. At $X(ZrO_2) > X_0$, tetragonal phase can be obtained as single phase.

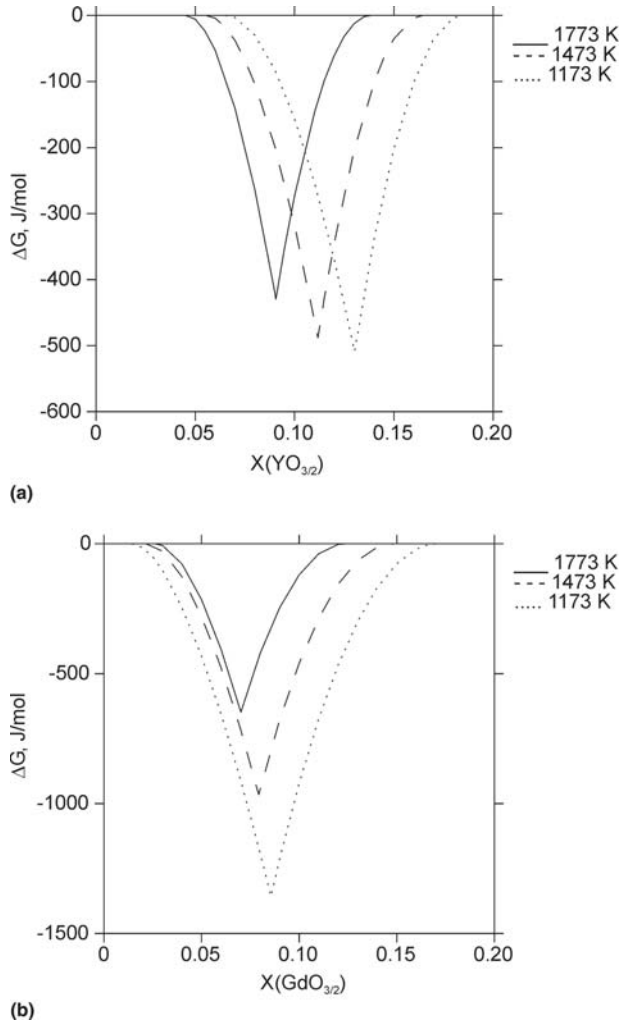

Fig. 8 The driving forces for partitioning of F and T metastable phases to F + T equilibrium phase assemblage calculated in the (a) ZrO_2-$YO_{3/2}$ and (b) ZrO_2-$GdO_{3/2}$ systems for temperatures of 1173, 1473, and 1773 K.

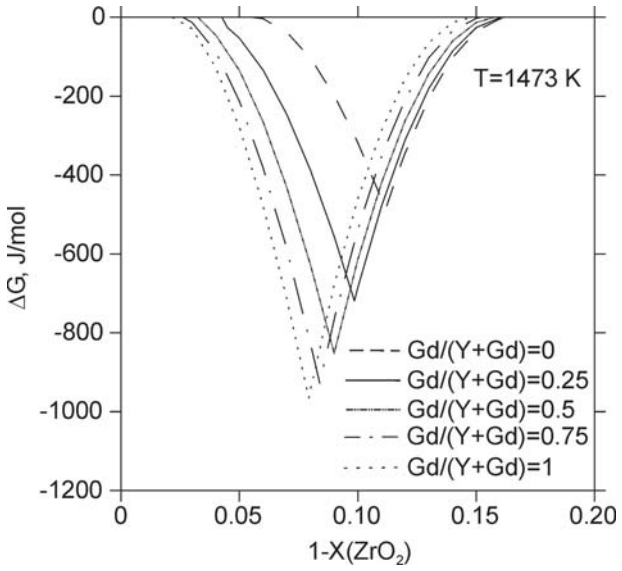

Fig. 9 Calculated driving force for partitioning of the metastable tetragonal and fluorite phases onto equilibrium two-phase field F + T in the ZrO_2-$GdO_{3/2}$-$YO_{3/2}$ system

These results are consistent with the trends observed in isothermal sections of the individual ternaries,[9-11,17] wherein the intersection of the tie-line separating the F + T + Al_2O_3 and F + Al_2O_3 fields moves to lower Al_2O_3 contents as the amount of stabilizer is increased and reflects the similarity in behavior between the two trivalent cations in solid solution.

It is further noted that the calculations predict the possibility that a garnet (LnAG) phase may form at the TBC/TGO interface for the higher Y/(Gd + Y) ratios within the range of total stabilizer content investigated, but not for the higher Gd content as expected from the absence of that phase in the $GdO_{3/2}$-$AlO_{3/2}$ binary (Fig. 1). The LnAG phase field in Fig. 3(a) and 4(a) would imply a (Gd + Y)/(Gd + Y + Zr) ratio that is not within the typical range of codoped TBCs at the temperatures of interest. (In essence, these fields evolve from the high Al_2O_3 corner of Fig. 1 as modest amounts of ZrO_2 are added.) Conversely, the formation of GAP by interaction between Al_2O_3 and more heavily loaded zirconias, for example, $Gd_2Zr_2O_7$, has been well documented,[6] but this was not included within the range of the calculations. In any event, the low cation diffusivity at the temperatures in which the LnAG phase is estimated to coexist with one of the zirconia polymorphs (<1000 K) in Fig. 3 and 4 makes it unlikely that this scenario can be realized in practice.

Of particular interest to thermal barrier coatings are tetragonal phases that exhibit adequate toughness without relying on martensitic transformations, which are disruptive to the integrity of the coating. The proposed toughening mechanism is one based on ferroelastic switching of tetragonal domains[27,28] and thus requires a structure that is tetragonal but not transformable to monoclinic (usually designated as t′). The lower bound of the range of desirable compositions is then defined by the intersection of the T_0(T/M) curve with ambient temperature, above which the tetragonal phase is nontransformable, and the upper bound by the intersection of the T_0(F/T) curve at the projected application temperature, above which the phase is no longer tetragonal but cubic. Reliable information on both equilibrium boundaries and T_0 curves such as that presented in Fig. 5 to 7 is thus of great interest in science-based design of new TBC compositions. For example, the curves in Fig. 7(a) determine the combination of Gd and Y doping added to ZrO_2 for which the thermodynamic preference switches from metastable tetragonal (more desirable) to metastable cubic (less desirable) at a given temperature. Substituting Gd for Y at a constant ZrO_2 content (horizontal line in Fig. 7a) decreases the maximum temperature at which the structure can remain tetragonal. Maintaining the Y content constant and substituting Gd for Zr (codoping), represented by a line of negative slope, further limits the range where t′ is stable, in agreement with the experimental results in work of Rebollo et al.[8] It is further noted from the comparison of

Fig. 5(a) and (c) and 6(a) that the intersection of the T_0(T/M) surface with ambient temperature is displaced to higher dopant concentrations as Gd is substituted for Y, further restricting the range in which a desirable t′ phase can be synthesized. (The calculation in Fig. 5(c) actually suggests that there is no viable thermodynamic range for a nontransformable phase that can be tetragonal at room temperature, but experiments suggest that this finding is overly restrictive and points to a need for additional work in this area.)

Because tetragonal phases with the right attributes are generally metastable in all zirconia systems doped with trivalent stabilizers,[6] their ability to retain their nontransformable nature is essential to their durability at high temperature. A critical factor in determining such kinetic stability is the driving force for partitioning of the metastable solid solution into the equilibrium tetragonal + cubic forms. The calculations made in the current study, Fig. 8 and 9, indicate that the maximal driving force takes more negative values in the ZrO_2-$GdO_{3/2}$ system than in the ZrO_2-$YO_{3/2}$ system in the temperature range of 1173 to 1773 K. This fact is in agreement with experimental studies of phase stability in this system.[8,29] The maximum driving force decreases with the temperature increase in both systems. However, in the ZrO_2-$YO_{3/2}$ system, the temperature dependence is not very pronounced, while in the ZrO_2-$GdO_{3/2}$ system the maximum driving force depends more strongly on temperature. With the substitution of Gd for Y the value of maximal driving force increases substantially. It is interesting to note that replacing half of the Y content with Gd leads to maximum driving force almost as high as in the ZrO_2-$GdO_{3/2}$ system. Moreover, for the typical stabilizer content in TBCs (7.6 mol%) the influence of Gd/(Y + Gd) ratio to driving force is most pronounced.

5. Conclusions

A thermodynamic database for the system ZrO_2-$YO_{3/2}$-$GdO_{3/2}$-$AlO_{3/2}$ system has been constructed from previously generated information on the integrating ternary and binary systems. While the Gibbs energy formulations used neglected higher-order interaction parameters as a first approximation, the results are quite consistent with current understanding arising from extensive experimental work on thermal barrier coatings. Of particular significance was the ability to generate data corresponding to metastable phases and their phase transformations, which are of primary importance in TBCs as well as the broader zirconia-based materials technology. Additional work is arguably needed to refine the models, especially with regard to the equilibrium fields involving the zirconia-based phases in the quaternary system and the T_0 curves that determine the desirable ranges of material design in TBC technology.

Acknowledgment

This study was undertaken as part of a broader program of international research collaboration on high-performance coatings (HIPERCOAT) jointly sponsored by the European Commission (GRD1-2000-30211) and the National Science Foundation (DMR-0099695). Collaborations between C.G. Levi and the MPI-MF were substantially enhanced through extended visits supported by the Alexander von Humboldt Foundation.

References

1. M.J. Maloney, Thermal Barrier Coating Systems and Materials, U.S. Patent 6,117,560, 2000
2. J. Wu, N.P. Padture, P.G. Klemens, M. Gell, E. Garcia, P. Miranzo, and M.I. Osendi, Thermal Conductivity of Ceramics in the ZrO_2-$GdO_{3/2}$ System, *J. Mat. Res.,* 2002, **17,** p 3193-3200
3. J.R. Nicholls, K.J. Lawson, A. Johnstone, and D.S. Rickerby, Methods to Reduce the Thermal Conductivity of EB-PVD TBCs, *Surf. Coat. Technol.,* 2002, **151-152,** p 383-391
4. D. Zhu and R.A. Miller, Thermal Conductivity and Sintering Behavior of Advanced Thermal Barrier Coatings, *Ceramic Engineering and Science Proceedings,* Vol 23, 2002, p 457-468
5. C.G. Levi, Emerging Materials and Processes for Thermal Barrier System, *Curr. Opin. Solid State Mater. Sci.,* 2004, **8,** p 77-91
6. R.M. Leckie, S. Kraemer, M. Ruhle, and C.G. Levi, Thermochemical Compatibility between Alumina and ZrO_2-$GdO_{3/2}$ Thermal Barrier Coatings, *Acta Mater.,* 2005, **53,** p 3281-3292
7. R. Vassen, F. Traeger, and D. Stoever, New Thermal Barrier Coatings Based on Pyrochlore/YSZ Double-Layer Systems, *Int. J. Appl. Ceram. Technol.,* 2004, **1,** p 351-361
8. N.R. Rebollo, O. Fabrichnaya, and C.G. Levi, Phase Stability of Y + Gd Codoped Zirconia, *Z. Metallkd.,* 2003, **95,** p 163-170
9. S. Lakiza, O. Fabrichnaya, Ch. Wang, M. Zinkevich, and F. Aldinger, Phase Diagram of the ZrO_2-Gd_2O_3-Al_2O_3 System, *J. Eur. Ceram. Soc.,* 2006, **26,** p 233-246
10. S. Lakiza, O. Fabrichnaya, M. Zinkevich, and F. Aldinger, Phase Relations in the ZrO_2-$YO_{3/2}$-$AlO_{3/2}$ System, *J. Alloys Compd.,* 2006, in press
11. O. Fabrichnaya, Ch. Wang, M. Zinkevich, C.G. Levi, and F. Aldinger, Phase Equilibria and Thermodynamic Properties of the ZrO_2-$GdO_{3/2}$-$YO_{3/2}$ System, *J. Phase Equilib. Diffus.,* 2005, **26,** p 591-604
12. M. Hillert, The Compound Energy Formalism, *J. Alloys Compd.,* 2001, **320,** p 161-176
13. T. Van Dijk, K.J. de Vries, and A.J. Burggraaff, Electrical Conductivity of Fluorite and Pyrochlore LnxZr1-xO2-x/2 (Ln = Gd,Nd) Solid Solutions, *Phys. Status Solidi (a),* 1980, **58,** p 115-125
14. T. Uehara, K. Koto, and F. Kanamaru, Stability and Antiphase Domain Structure of the Pyrochlore Solid Solutions in the ZrO_2-Gd_2O_3 System, *Solid State Ionics,* 1987, **23,** p 137-143
15. A. Negro and I. Amato, Investigation of Zirconia-Gadolinia System, *J. Less-Common Met.,* 1972, **26,** p 81-88
16. S. Lakiza and L.M. Lopato, Stable and Metastable Phase Relations in the System Alumina-Zirconia-Yttria, *J. Am. Ceram. Soc.,* 1997, **80,** p 893-902
17. O. Fabrichnaya and F. Aldinger, Assessment of Thermodynamic Parameters in the System ZrO_2-Y_2O_3-Al_2O_3, *Z. Metallkd.,* 2004, **95,** p 27-39
18. S. Lakiza, The System $GdO_{3/2}$-$YO_{3/2}$-$AlO_{3/2}$, private communication
19. M. Ruehle, N. Claussen, and A.H. Heuer, Microstructural Studies of Y_2O_3 Containing Tetragonal ZrO_2 Polycrystals (Y-TZP), in *Science and Technology of Zirconia II,* N. Claussen,

M. Rühle, and A.H. Heuer, Ed., The American Ceramic Society, 1984, p 352-370
20. A.G. Evans and R.M. Cannon, Toughening of Brittle Solids by Martensitic Transformations, *Acta Mater.,* 1986, **34**(5), p 761-800
21. A.H. Heuer, R. Chaim, and V. Lanteri, Review: Phase Transformations and Microstructural Characterization of Alloys in the System Y_2O_3-ZrO_2, in *Science and Technology of Zirconia III,* S. Somiya, N. Yamamoto, and H. Yanagida, Ed., The American Ceramic Society, 1988, p 3-20
22. V. Lughi, "Phase Stability of Yttria-Stabilized Zirconia for Thermal Barrier Coating Applications," MS Thesis, University of California, Santa Barbara, CA, 2005
23. M. Yashima, N. Ishizawa, and M. Yoshimura, High Temperature X-Ray Diffraction Study on Cubic-Tetragonal Phase Transition in the ZrO_2-$RO_{1.5}$ Systems (R:Rare Earths), in *Science and Technology of Zirconia V,* S.P.S. Badwal, M.J. Bannister, R.H.J. Hannink, Ed., Technomic, Lancaster, PA, 1993, p 125-135
24. R.S. Mullin, W.P. Allen, M.L. Gell, R.H. Barkalow, A.A. Noetzel, J.W. Appleby, and A.S. Khan, Multiple Nanolayer Coating System, United Technologies Corp., Hartford, CT, 1997
25. R.W. Bruce, J.C. Schaeffer, M.A. Rosenzweig, R. Viguie, D.V. Rigney, A.F. Maricocchi, D.J. Wortman, and B.A. Nagaraj, Thermal Barrier Coating Resistant to Erosion and Impact by Particulate Matter, General Electric Co., Cincinnati, OH, 1997
26. W.C. Hasz, M.P. Borom, and C.A. Johnson, Protection of Thermal Barrier Coating with an Impermeable Barrier Coating, General Electric Co., Schenectady, NY, 1999
27. A.V. Virkar, Role of Ferroelasticity in Toughening of Zirconia Ceramics, *Key Eng. Mater.,* 1998, **153-154,** p 183-210
28. D. Baither, M. Bartsch, B. Baufeld, A. Tikhonovsky, F.A.M. Rühle, and U. Messerschmidt, Ferroelastic and Plastic Deformation of t′-Zirconia Single Crystals, *J. Am. Ceram. Soc.,* 2001, **84**(8), p 1755-1762
29. N.R. Rebollo, "Phase Stability of t′-Zirconia with Trivalent Oxide Additions for Use in Thermal Barrier Coatings," Ph.D. Dissertation in Materials, University of California, Santa Barbara, CA, 2005